ARTICLE

BIOTECHNOLOGY and BIOENGINEERING

3D Collagen Cultures Under Well-Defined Dynamic Strain: A Novel Strain Device With a Porous Elastomeric Support

Alice A. Tomei,[1] Federica Boschetti,[2] Francesca Gervaso,[3] Melody A. Swartz[1]

[1]Institute of Bioengineering, École Polytechnique Fédérale de Lausanne (EPFL), SV-LMBM, Station 15, 1015 Lausanne, Switzerland; telephone: +41-21-693-9686; fax: +41-21-693-9685; e-mail: melody.swartz@epfl.ch

[2]Department of Structural Engineering, Politecnico di Milano, Milan, Italy

[3]Biomaterials Science Laboratory, Dipartimento di Ingegneria dell'Innovazione, Università del Salento, Lecce, Italy

Received 12 September 2008; revision received 28 November 2008; accepted 12 December 2008

Published online 16 December 2008 in Wiley InterScience (www.interscience.wiley.com). DOI 10.1002/bit.22236

ABSTRACT: The field of mechanobiology has grown tremendously in the past few decades, and it is now well accepted that dynamic stresses and strains can impact cell and tissue organization, cell–cell and cell–matrix communication, matrix remodeling, cell proliferation and apoptosis, cell migration, and many other cell behaviors in both physiological and pathophysiological situations. Natural reconstituted matrices like collagen and fibrin are often used for three-dimensional (3D) mechanobiology studies because they naturally form fibrous architectures and are rich in cell adhesion sites; however, they are physically weak and typically contain >99% water, making it difficult to apply dynamic stresses to them in a truly 3D context. Here we present a composite matrix and strain device that can support natural matrices within a macroporous elastic structure of polyurethane. We characterize this system both in terms of its mechanical behavior and its ability to support the growth and in vivo-like behaviors of primary human lung fibroblasts cultured in collagen. The porous polyurethane was created with highly interconnected pores in the hundreds of μm size scale, so that while it did not affect cell behavior in the collagen gel within the pores, it could control the overall elastic behavior of the entire tissue culture system. In this way, a well-defined dynamic strain could be imposed on the 3D collagen and cells within the collagen for several days (with elastic recoil driven by the polyurethane) without the typical matrix contraction by fibroblasts when cultured in 3D collagen gels. We show lung fibroblast-to-myofibroblast differentiation under 30%, 0.1 Hz dynamic strain to validate the model and demonstrate its usefulness for a wide range of tissue engineering applications.

Biotechnol. Bioeng. 2009;103: 217–225.

KEYWORDS: mechanical stress; mechanobiology; in vitro; fibroblast; collagen

Introduction

Research in tissue engineering aims to develop design principles for functional tissue replacement in vivo or for building three-dimensional (3D) model systems to study human tissue function and pathobiology (Griffith and Swartz, 2006). It is increasingly appreciated that mechanical forces act as important functional cues affecting tissue organization and behavior (Grodzinsky et al., 2000; Humphrey, 2008; Ingber, 2003; Pedersen and Swartz, 2005; Sacks and Yoganathan, 2007; Setton and Chen, 2004; Vanepps and Vorp, 2007; Wirtz and Dobbs, 2000). Indeed, 3D tissue culture under well-defined mechanical conditions is becoming standard in tissue engineering of bone, cartilage, blood vessels, and cardiac muscle (Isenberg et al., 2006; Liu, 1999; Rivron et al., 2008; Rutkowski and Swartz, 2007; Shieh and Athanasiou, 2003; Sorkin et al., 2004). Furthermore, mechanical stresses have been shown to affect tissue organization and remodeling in 3D in vitro tissue culture models of the airway wall (Choe et al., 2006; Tschumperlin and Drazen, 2006), capillary morphogenesis (Helm et al., 2005; Ng et al., 2004), tumorigenesis (Paszek et al., 2005; Wozniak et al., 2003), and stem cell differentiation (Engler et al., 2006; Park et al., 2007), among others.

In most tissues, the main component of the extracellular matrix is type I collagen and thus it is the most widely employed extracellular matrix in vitro (Griffith and Swartz,

Correspondence to: M.A. Swartz
Contract grant sponsor: Swiss National Science Foundation
Contract grant number: 107602; 310010

2006). However, type I collagen gels used in vitro (typically reconstituted from rat tail tendon) for 3D culture have a much lower collagen density than that typically seen in vivo and are extremely weak mechanically. For this reason, it is difficult to use collagen and other natural reconstituted matrices like fibrin for in vitro 3D mechanobiology experiments, particularly for dynamic strains, due to matrix contraction (e.g., fibroblasts and smooth muscle cells can contract a matrix to a fraction of its original size) and because such reconstituted collagen and fibrin cannot maintain any residual stress when compressed or stretched (Pedersen and Swartz, 2005; Roeder et al., 2002). Thus, reproducing relevant biophysical environments in 3D culture systems with such soft matrices is technically challenging (Brown, 2000). For tensile strain application, cells have been cultured in a matrix that is polymerized atop a silicon membrane and then strained by applying a negative pressure (Breen, 2000) or by elongating the membrane (Butcher et al., 2006; Joung et al., 2006), or within an extracellular matrix that is anchored at one end and stretched at the other (Berry et al., 2003; Liu et al., 1999a; Raeber et al., 2008). Compression loading systems include direct confined or unconfined platen abutment (Brown, 2000) and sponge-supported systems (Choe et al., 2006). However, these methods often suffer from ill-defined strain distributions, difficulty in setup and reproducibility, and adaptation to different types of mechanical conditions.

Here we present a new composite matrix for 3D mechanobiology experiments and a novel strain device for culturing soft tissue cultures under well-defined dynamic strain conditions. Since the collagen component is critical for cell response, we reinforce it with a porous elastomeric sponge with pores (50–600 μm) that are an order of magnitude larger than the cells. In this way, we can maintain the cells in the collagen environment while the overall stress/strain relationships are governed by the elastomeric sponge rather than the collagen. Specifically, we created a porous polyurethane (PU) sponge using alginate beads to create pores; the PU is biocompatible and hydrophilic and displays an elastic modulus that is orders of magnitude higher than that of reconstituted type I collagen. Even without external strain application, the PU–collagen composite resists contraction by fibroblasts or other contractile cells. The composite matrix is cast into a dynamic strain device that is simple to set up and that can be cultured in an incubator under constant dynamic strain for indefinite periods of time.

Materials and Methods

Polyurethane Sponge Fabrication

Alginate beads, with diameters of 50–500 μm, were prepared by extruding a solution of 2% sodium alginate (Fluka, Buchs, Switzerland) in distilled water (dH_2O) through a 25 G needle fitted with a syringe into a solution of 102 mM $CaCl_2$ in 0.9% NaCl (Fluka). After 1 h the beads were vacuum filtered and air-dried. Dried beads were packed in the 10 mm × 20 mm × 5 mm sponge-casting device (Fig. 1a, Step 1) and a 25 mg/mL solution of PU (Pellethane 2363-80A; Dow Plastics, Midland, MI) in *N*-methyl-pyrrolidone (NMP; Fluka) was poured onto the beads and allowed to penetrate into the spaces between the packed beads. After 90 min, the NMP solvent was removed from the PU solution by solvent exchange with dH_2O (Fig. 1a, Step 2). The alginate beads were then dissolved with 0.5 M citric acid solution. The resulting PU sponge, with a final size equivalent to that of the casting device (10 mm × 20 mm × 5 mm), was rinsed over 3 days in dH_2O and autoclaved in

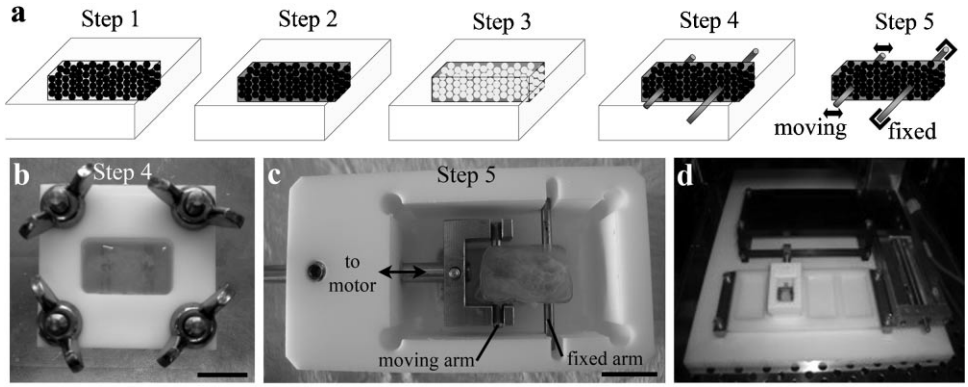

Figure 1. Strain device setup. **a**: Schematic outlining the production of the composite matrix. Step 1—pack alginate beads within mold. Step 2—pour liquid polyurethane (PU) in the interstices of the alginate beads; let polymerize at 37°C, 5% CO_2. Step 3—dissolve alginate beads to create pores, and thoroughly rinse the PU sponge. Step 4—insert pins into the sponge casting device and add cell-seeded collagen (or other biopolymer) solution to the PU sponge to saturate the macropores; let polymerize. Step 5—transfer the PU–collagen composite matrix, with pins intact, to the strain device frame. One pin is fixed to the frame and the other one is attached to the movable arm, which is connected to the linear motor. **b**: Picture of PU–collagen composite in Step 4 (bar = 10 mm). **c**: Picture of the composite matrix within the strain device from Step 5 (bar = 10 mm). **d**: Picture of the matrix within the strain device, connected to the linear motor, inside a standard cell culture incubator.

PBS. The PU sponge was modified from a previously published method (Bezuidenhout et al., 2002).

Mechanical Properties of the PU–Collagen Matrix

Mechanical tests were performed using an electromagnetic testing machine (Enduratec ELF3200; Bose Corporation, Eden Prairie, MN), equipped with a load cell of 22 N, under displacement control. Unconfined tests were performed by placing the specimen in a PMMA chamber and applying compressive strain by a non-porous PMMA indenter. The samples were made with a 10 mm diameter. Sample thickness was measured from the position of the testing machine actuator, after imposing a preload of approximately 0.3 kPa. Throughout the measurements, samples were immersed in PBS. The samples underwent the following tests: (i) a 5% step-wise compression (up to 15% strain), followed by (ii) 15% static compression, followed by (iii) dynamic compression at 15% strain amplitude. (i) The step-wise compression consisted of a series of three strain ramps, each 5% of the sample thickness, at a velocity of 0.01 mm/s, followed by stress relaxation to equilibrium. (ii) The 15% strain compression consisted of a single strain ramp of 15% followed by stress relaxation to equilibrium. (iii) The dynamic test consisted of sinusoidal 15% compression at 0.01, 0.1, or 1 Hz. From the equilibrium stress–strain data, we calculated the Young's modulus E under the hypothesis of linear poroelasticity, since the elastomeric sponge by itself displayed linear elastic behavior and the collagen solution contributed only to the hydraulic permeability of the composite.

The permeability was evaluated by using a custom-made device consisting of two coaxial cylinders and a capillary flow meter (Boschetti et al., 2006). The sample was placed on a porous polyethylene filter with an O-ring to prevent flow from bypassing the sample, and PBS was imposed through the sample using pressure heads of 18–50 cmH_2O. The hydraulic permeability was calculated using Darcy's law according to the measured flow velocities.

To evaluate the Poisson ratio, the specimens were placed in a transparent chamber and subjected to a 15% axial strain while transversely observed through a stereomicroscope (SMZ800; Nikon, Tokyo, Japan). Images were acquired by a digital camera (Nikon DS-5M) connected to the microscope and elaborated to obtain radial strain from the lateral expansion. The Poisson ratio was then calculated as axial to radial strain.

Cell Culture and Strain Device Setup

Human fetal lung fibroblasts (IMR-90; ATCC, Manassas, VA) were expanded in α-modified minimum essential Eagle's medium (α-MEM; Gibco, Carlsbad, CA) supplemented with 10% FBS (Invitrogen, Paisley, UK) and 1% penicillin–streptomycin–amphotericin (Invitrogen), and used between passages 16 and 19. They were suspended at 500,000 cells/mL in 2.5 mg/mL type I collagen (BD Biosciences, Basel, Switzerland).

After rinsing, the PU sponge was placed back into the sponge-casting device and two fine stainless steel rods (16 G needles) were inserted at a distance of 10 mm from each other and 5 mm from the borders of the sponge (Fig. 1b); these rods were to be used later for strain application to the sponge. The device was sealed and the collagen–cell solution was poured into the sponge to saturate the macropores (Fig. 1a, Step 4). After polymerization at 37°C, 5% CO_2, the composite matrix was placed in the strain device frame (Fig. 1a, Step 5, and c) and connected to the linear step motor by a platform that was fixed to both the motor and the piston (Fig. 1d). For collagen-only samples, the PU sponge was not added, and the collagen was poured directly into the casting device. All cultures were maintained in a humidified 37°C, 5% CO_2 incubator for the duration of the culture.

Computational Estimates of Flow and Strain Distributions

The strain and flow velocity distributions within the PU–collagen sponge were estimated with a computational model of the experimental system, developed using a commercial finite element code (ABAQUS v.6.8). The porous medium representing the composite matrix was considered as a biphasic material and the classic consolidation theory was adopted to describe its behavior. Large deformation theory was employed in the finite element formulation to obtain the numerical solution.

The hydrated PU–collagen sponge was modeled as a biphasic material where the solid component was the poroelastic PU–collagen composite and the fluid component represented the culture medium. The solid phase was considered a porous, incompressible, isotropic, linear elastic material characterized by the Young's modulus E and Poisson ratio ν as determined in the Mechanical Properties of the PU–Collagen Matrix Section; the fluid was considered incompressible and its interaction with the solid phase characterized by the hydraulic permeability K and the porosity ϕ of the solid (i.e., PU-collagen composite).

A parallelepiped (20 mm × 10 mm × 5 mm) with two cylindrical holes representing the fixed and moving posts (Fig. 4a) was discretized with 9060 pore fluid elements (C3D8P; Fig. 4b). The nodes lying on the surface of one of the two holes were constrained in the three directions in order to simulate the fixed post; moreover, the pore pressure was set equal to zero at all surfaces of the PU–collagen sponge. A 30% compression ramp at 0.1 Hz was imposed to the nodes of the free hole surface in the x-direction, in order to simulate the experimental conditions imposed on the matrix between the two needles (Fig. 4c).

The results were analyzed in terms of strain and fluid velocity in the principal directions at the beginning and at

the end of the cyclic compression, after a few cycles were run to stabilize results.

Dynamic Strain Application

The 3D culture of human fetal lung fibroblasts in the composite matrix was created in the strain device described above, and a dynamic compression regimen of 30% was applied to the composite matrix at a frequency of 0.1 Hz for 12 h at a constant strain rate (5 s compression followed by 5 s relaxation, both at 3%/s) inside a 5% CO_2, 37°C incubator by a linear motor connected to an electronic controller (Cosmos, Velmex, Bloomfield, NY).

Fibroblast Characterization for Actin and α-Smooth Muscle Actin

Samples were fixed by immersion in 4% paraformaldehyde in PBS for 2 h at room temperature, rinsed with PBS, and permeabilized in 0.1% Triton for 5 min. AlexaFluor 488-conjugated phalloidin (1:50, Invitrogen, Carlsbad, CA) was used to examine the F-actin cytoskeletal structure and the alignment of fibroblast cells while Cy3-conjugated anti-α-smooth muscle actin antibody (Fluka) was used to examine myofibroblast differentiation. 4′,6-diamidino-2-phenylindole (DAPI)-containing mounting medium (Vectashield H-1200; Vectorlabs, Burlingame, CA) was used to stain the nuclei and preserve the sample fluorescence. Images were taken using a Zeiss Axiovert 200M fluorescence microscope with AxioCam MRm camera and a Zeiss LSM510 META Zeiss laser scanning confocal microscope (Carl Zeiss AG, Feldbach, Switzerland). Imaris (Bitplane, Zurich, Switzerland) was used for image quantification of 3D confocal stacks. To determine α-smooth muscle actin (α-SMA) and F-actin expression within the fibroblasts, average intensity and total Cy3+ and FITC+ volumes were determined in at least five different fields of each sample and normalized to cell number. A one-tailed, unpaired Mann–Whitney test was used to determine statistical significance between static and strained conditions.

Results and Discussion

Mechanical Properties of the PU Sponge–Collagen Composite Matrix

By phase contrast microscopy we found that the PU sponge had a structure of highly interconnected macropores with narrow walls between pores and a broad pore size distribution between 50 and 600 μm (Fig. 2a–c). Under quasi-static compression, the Young's modulus was found to be independent of strain within the range of 5–15% (Fig. 2d, $n=4$), while the dynamic Young's modulus at 15% strain at 0.1 and 1 Hz was roughly twice that value (Fig. 2e, $n=4$). Since the collagen gel by itself could not support a residual strain, the elastic modulus of the composite was governed by the PU sponge.

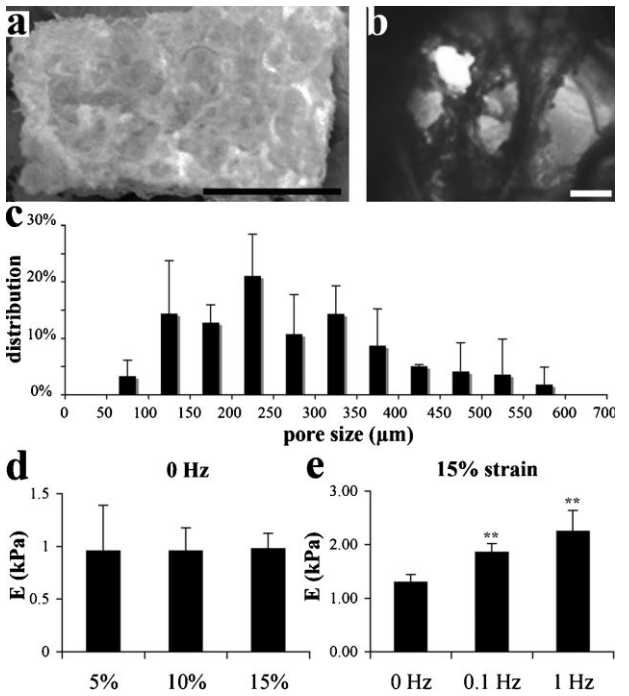

Figure 2. Mechanical characterization of the polyurethane (PU) sponge–collagen composite matrix. **a** and **b**: Phase contrast micrographs of the PU sponge show a structure of highly interconnected macropores with narrow walls between pores. Scale bars—a: 10 mm and b: 200 μm. **c**: Pore sizes were distributed between 50 and 600 μm ($n=3$). **d**: Under quasi-static compression, the Young's modulus was independent of strain within the range of 5–15% ($n=4$). **e**: The dynamic Young's modulus at 15% strain at 0.1 and 1 Hz was roughly twice that at 0 Hz ($P=0.002$, $n=4$).

The collagen gel dominated the overall hydraulic resistance of the composite, since it was orders of magnitude less permeable than the porous PU sponge. We found the permeability of the composite matrix to be 7.6×10^{-9} cm^2 and the Poisson coefficient to be 0.1, which is consistent with previous measurements of reconstituted collagen gels (Ramanujan et al., 2002; Swartz and Fleury, 2007).

3D Culture of Lung Fibroblasts in the PU–Collagen Composite Matrix

We found that the PU sponge–collagen composite matrix supported the long-term 3D culture of dermal and lung fibroblasts as well as several tumor cell lines with no apparent differences in morphology compared to culture in collagen alone (Fig. 3a). Also, without the PU support, cells cultured in collagen-only matrices contracted their matrices quickly and excessively (~75% of original area after 7 days) while cells in the PU–collagen composite maintained their

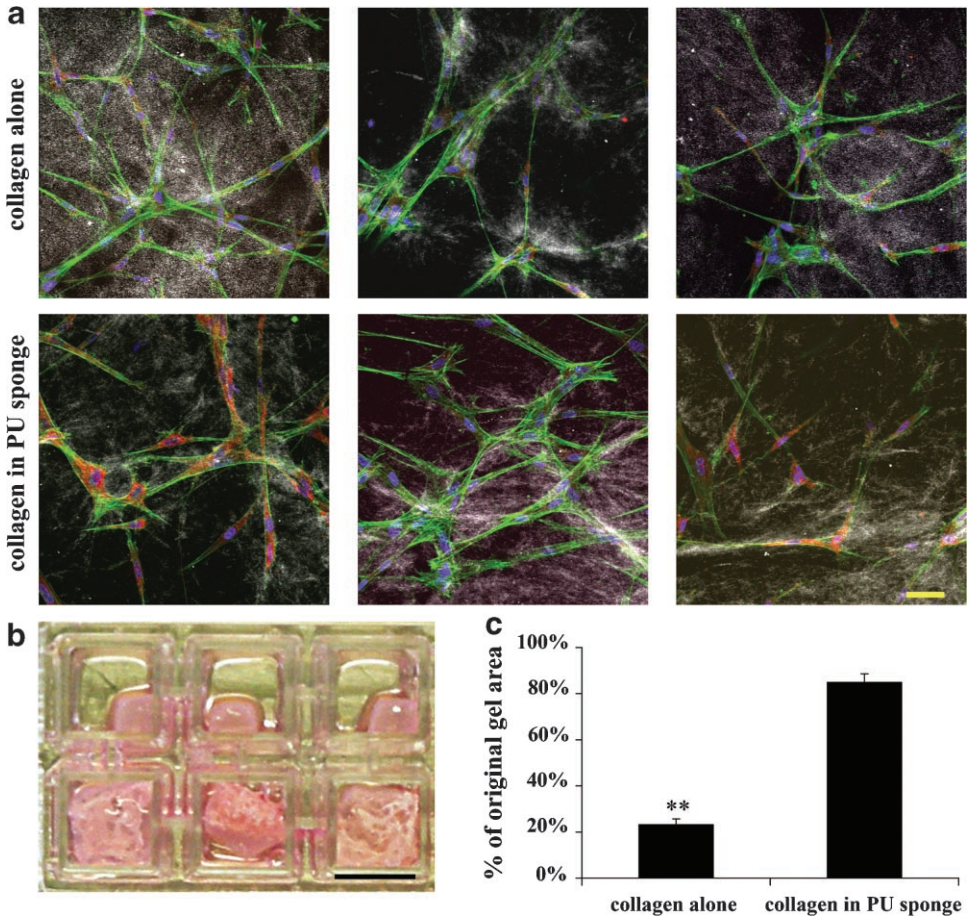

Figure 3. Three-dimensional culture of lung fibroblasts in the polyurethane (PU)–collagen composite matrix versus collagen alone. **a**: The PU sponge–collagen composite matrix supported the long-term 3D culture of lung fibroblasts similar to when cultured in collagen alone. Fibroblast differentiation to myofibroblasts, as indicated by α-smooth muscle actin (α-SMA) expression (red), was visibly enhanced in the composite matrix. Nuclei: blue (DAPI). Scale bar = 50 μm. **b** and **c**: Collagen alone matrices (**b**, top row) did not allow long-term culture of lung fibroblasts since the cells contracted the matrix to 23% (±2%) of its original area, while collagen in the PU sponge matrices (**b**, bottom row) were able to counteract cell contraction during culture ($P = 0.003$). Scale bar = 8 mm.

original volume over the same culture time (Fig. 3b and c). Furthermore, fibroblast differentiation to myofibroblasts, as indicated by α-SMA expression, was visibly enhanced in the composite matrix (Fig. 3a), suggesting that the composite matrix, from the perspective of the cell, could better resist cell contractile forces and promote stress fiber formation and myofibroblast differentiation (Hinz, 2007).

Computational Strain and Flow Profiles of the Composite Matrix Under Dynamic Strain

The stress relaxation time for the composite subjected to unconfined compression was in the range of 100 s. If the dynamic strain period (inverse of strain frequency) is equal or greater than the relaxation time of the composite material, the material will be in quasi-equilibrium and the strain should be uniformly distributed within the material. In the experiments described here, the strain period (10 s) was smaller than the relaxation time of the material, so we would expect the strain profile to not be uniformly distributed. We also would expect that fluid flows in and out through the free sides of the matrix as it undergoes dynamic strain, as described in Soulhat et al. (1999).

To estimate and visualize the strain and flow profiles within the culture system, we modeled the dynamic compression at limits in the strain compression cycle (30% and 0%) using finite element modeling software. Porosity ϕ was set at 99.7%, that of the 3 mg/mL reconstituted collagen matrix, and the other parameters were found above: $E = 1.9$ KPa, $\nu = 0.1$, and $K = 10^{-6}$ mm^2.

Figure 4 shows the 3D flow (v) and strain ($\ln \lambda$, where λ is defined as $\lambda = l/l_0$ according to the large deformation theory) distributions within the matrix at the end of the loading phase (30% compression) and at the end of the unloading phase (0% compression). Such results are obtained after a few load–unload cycles run to reach stable results. As underlined by the shape of 3D and 2D images for 0% compression, the matrix volume is reduced at the end of the unloading phase due to fluid exudation during the

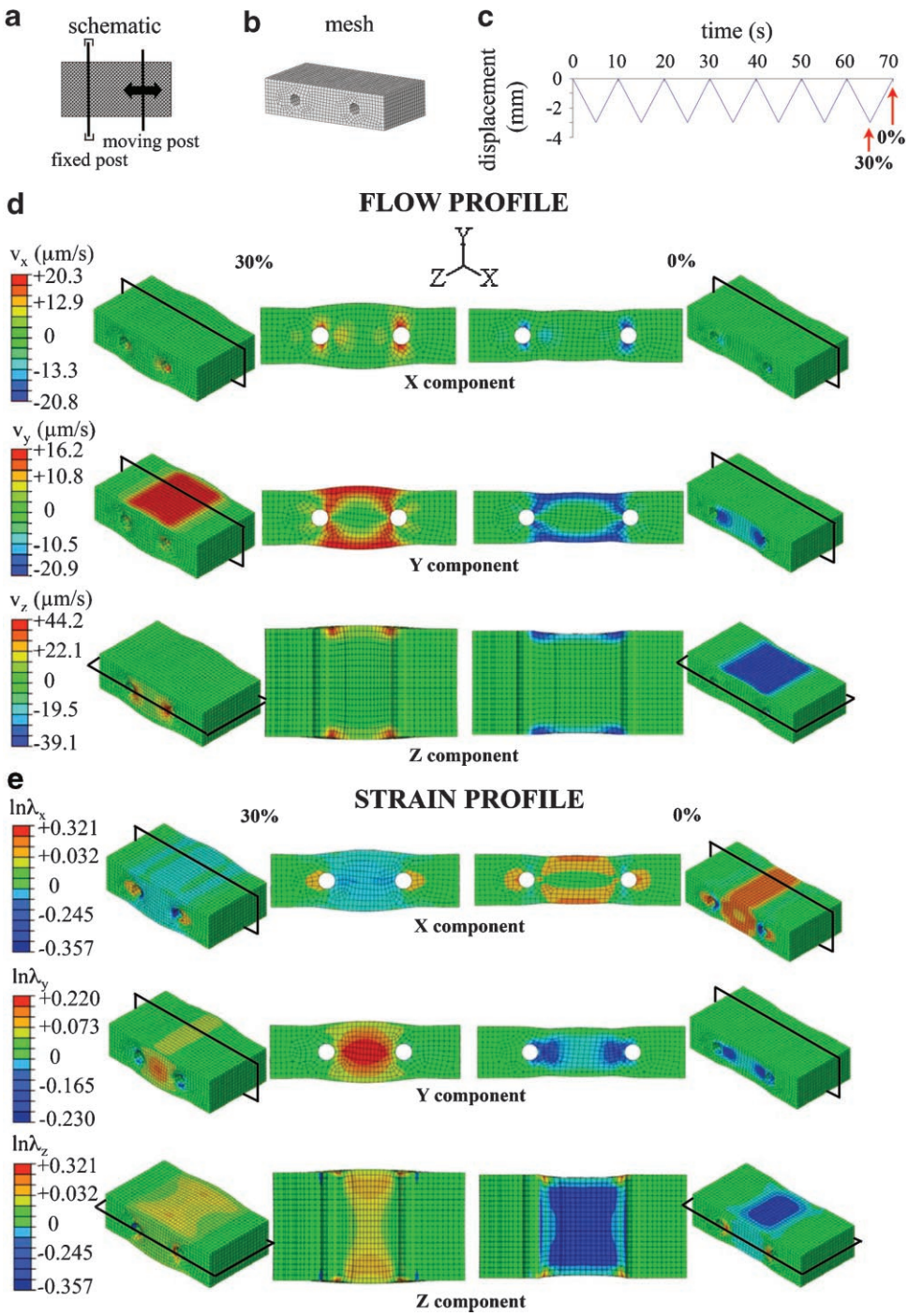

Figure 4. Numerical results for flow and strain profiles within the porous polyurethane–collagen matrix under dynamic compression. **a**: Schematic of the sponge with moving and fixed posts. **b**: Meshed geometrical model of the sponge with holes representing the posts. **c**: Strain curve applied to the material. Numerical results are taken from the last cycles. **d** and **e**: Flow and strain profiles. Left: end of the loading phase (30% compression); right: end of the unloading phase (0% compression). Green represents zero flow or zero strain, red represents outflow or tension, and blue color represents inflow or compression; values are shown on the corresponding scales for each parameter (flow, *v*, or strain, ln λ) and each direction (*x*, *y*, *z*). Two-dimensional sections are taken in the middle of the 3D geometry. **d**: Flow profile: fluid is exuded (any direction) at the end of the loading phase and re-adsorbed at the end of the unloading phase. **e**: Strain profile: the sponge is compressed along the loading direction (*x*) and in tension along the other directions at the end of the loading phase, the opposite occurs at the end of the unloading phase.

loading phase. Fluid exits the sponge during compression (red color for flow profile in Fig. 4d) and is partly re-adsorbed (blue color for flow profile in Fig. 4d) during the unloading phase. The sponge is compressed in the *x*-direction at the end of the loading phase (Fig. 4e, top row left). At the end of the unloading phase the sponge is slightly in tension along the *x*-direction (Fig. 4e, top row right) as a consequence of fluid loss and volume reduction.

Dynamic Strain Application to Fibroblasts

We tested the strain device with human lung fibroblasts as a model of interstitial tissue, since fibroblasts are among the most widely studied in terms of their response to mechanical stress. First, we found that under dynamic conditions fibroblasts were more widely spread and had a more noticeable spindle-shaped morphology than those in static conditions. Near the edges of the matrix, we found cells aligned perpendicular to the expected direction of fluid flow and with the imposed strain direction. Because flow and strain are necessarily coupled, we could not differentiate specific responses to flow versus strain, but this alignment was consistent with our previous studies showing that fibroblasts in collagen gels undergoing interstitial flow alone (without matrix compression) align perpendicular to the direction of flow (Ng and Swartz, 2003, 2006). We note that most of the previous work on fibroblast mechanobiology has been done by applying either tension or confined compression to the cells (Eastwood et al., 1998; Grinnell, 2003; Liu et al., 1999b; Wang et al., 2007), with tensional forces driving alignment of cells parallel to the strain direction (Henshaw et al., 2006; Voge et al., 2008); this is consistent with our findings. This demonstrates the usefulness of this model system for mechanobiology involving 3D dynamic compressive or tensile stresses.

We also found that the cells had increased expression of α-SMA in dynamic conditions compared to static controls (Fig. 5), indicating transition to a myofibroblast phenotype. Our previous studies showed that interstitial flow can induce myofibroblast differentiation (Ng et al., 2005). This was dependent on both integrin $\alpha_1\beta_1$ and TGF-β_1, which is consistent with a more recent report that mechanical stress can directly activate TGF-β_1 from stores in the extracellular matrix (Wipff et al., 2007), since it is secreted by fibroblasts in an inactive matrix-binding form that must then be activated to induce their differentiation. Thus, this is a likely mechanism for the dynamic strain-induced myofibroblast

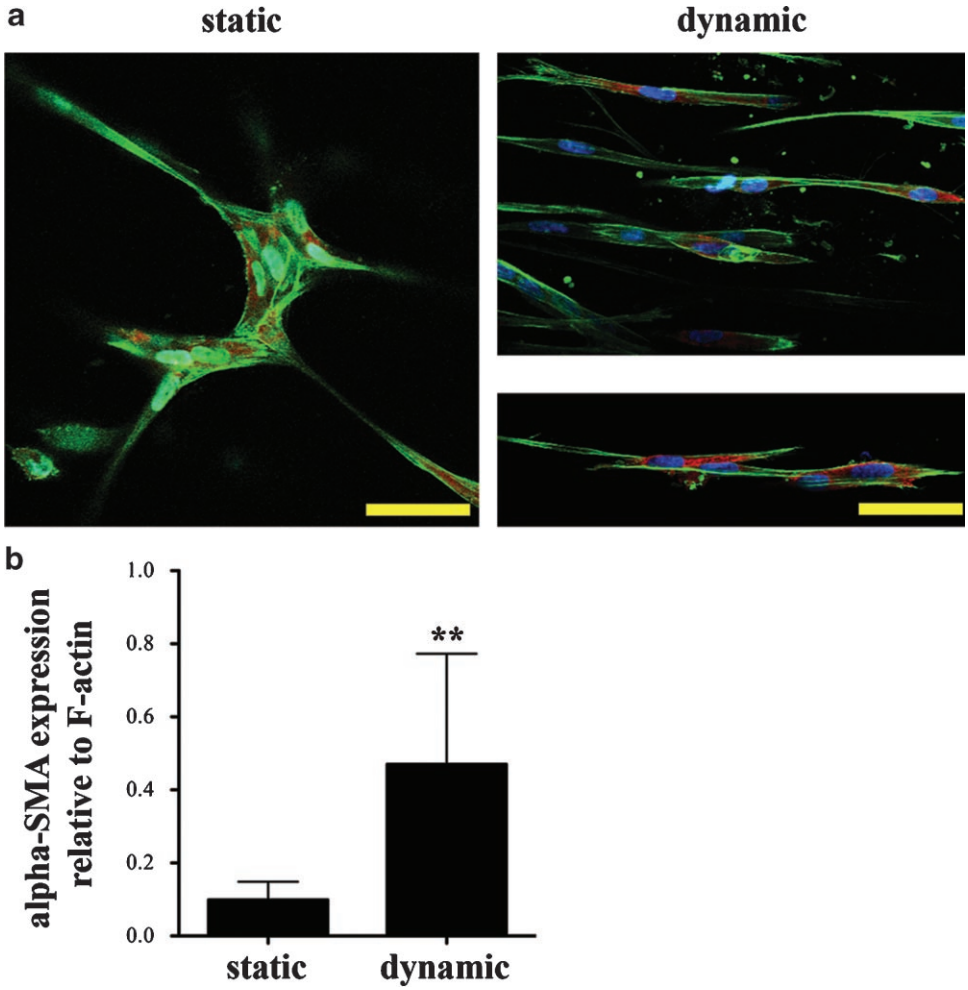

Figure 5. Dynamic strain in the composite matrix induced myofibroblast differentiation of lung fibroblasts. **a**: Alpha-smooth muscle actin (α-SMA) (red) immunostaining in confocal images of whole mounts. **b**: Lung fibroblasts showed increased expression of α-SMA in dynamic compared to static conditions by image quantification ($P = 0.004$). Nuclei: blue (DAPI); bars = 50 μm.

differentiation that we saw here, used to demonstrate that indeed mechanical strain-induced cell behaviors can be recapitulated in our device.

Conclusions

We have presented a unique composite matrix and strain device to culture different cells types in a physiological, mechanically dynamic 3D environment. Our composite matrix can readily withstand fibroblast contractile force, providing a stiff, elastic 3D environment while at the same time allowing the cells to be embedded in a soft biopolymer like collagen. The elastic sponge has large enough pores so that the cell microenvironment is the soft biopolymer, is stiff enough to prevent contraction, is elastic enough to readily undergo dynamic strain in a reproducible and characterizable way, and is biocompatible for long-term cell culture. Because the stress–strain behavior is controlled by the PU sponge and the viscous behavior controlled by the biopolymer, strain can be imparted to embedded cells without inducing artificial stress concentration and matrix damage and allowing for the study of both the direct effect of stress and the indirect effect of strain-induced flow through the matrix. The system is straightforward to set up and highly reproducible, and it can easily be extended to other cell types and hydrated matrices such as fibrin, alginate, and PEG.

We are grateful to Brandon Dixon and Adrian Shieh for helpful technical advice and Deon Bezuidenhout and Jeffrey Hubbell for advice on the PU sponge. This work was funded by the Swiss National Science Foundation (107602 and 310010).

References

Berry CC, Shelton JC, Bader DL, Lee DA. 2003. Influence of external uniaxial cyclic strain on oriented fibroblast-seeded collagen gels. Tissue Eng 9(4):613–624.

Bezuidenhout D, Davies N, Zilla P. 2002. Effect of well defined dodecahedral porosity on inflammation and angiogenesis. ASAIO J 48(5):465–471.

Boschetti F, Gervaso F, Pennati G, Peretti GM, Vena P, Dubini G. 2006. Poroelastic numerical modelling of natural and engineered cartilage based on in vitro tests. Biorheology 43(3–4):235–247.

Breen EC. 2000. Mechanical strain increases type I collagen expression in pulmonary fibroblasts in vitro. J Appl Physiol 88(1):203–209.

Brown TD. 2000. Techniques for mechanical stimulation of cells in vitro: A review. J Biomech 33(1):3–14.

Butcher JT, Barrett BC, Nerem RM. 2006. Equibiaxial strain stimulates fibroblastic phenotype shift in smooth muscle cells in an engineered tissue model of the aortic wall. Biomaterials 27(30):5252–5258.

Choe MM, Sporn PH, Swartz MA. 2006. Extracellular matrix remodeling by dynamic strain in a three-dimensional tissue-engineered human airway wall model. Am J Respir Cell Mol Biol 35(3):306–313.

Eastwood M, McGrouther DA, Brown RA. 1998. Fibroblast responses to mechanical forces. Proc Inst Mech Eng [H] 212(2):85–92.

Engler AJ, Sen S, Sweeney HL, Discher DE. 2006. Matrix elasticity directs stem cell lineage specification. Cell 126(4):677–689.

Griffith LG, Swartz MA. 2006. Capturing complex 3D tissue physiology in vitro. Nat Rev Mol Cell Biol 7(3):211–224.

Grinnell F. 2003. Fibroblast biology in three-dimensional collagen matrices. Trends Cell Biol 13(5):264–269.

Grodzinsky AJ, Levenston ME, Jin M, Frank EH. 2000. Cartilage tissue remodeling in response to mechanical forces. Annu Rev Biomed Eng 2: 691–713.

Helm CL, Fleury ME, Zisch AH, Boschetti F, Swartz MA. 2005. Synergy between interstitial flow and VEGF directs capillary morphogenesis in vitro through a gradient amplification mechanism. Proc Natl Acad Sci USA 102(44):15779–15784.

Henshaw DR, Attia E, Bhargava M, Hannafin JA. 2006. Canine ACL fibroblast integrin expression and cell alignment in response to cyclic tensile strain in three-dimensional collagen gels. J Orthop Res 24(3): 481–490.

Hinz B. 2007. Formation and function of the myofibroblast during tissue repair. J Invest Dermatol 127(3):526–537.

Humphrey JD. 2008. Mechanisms of arterial remodeling in hypertension: Coupled roles of wall shear and intramural stress. Hypertension 52(2): 195–200.

Ingber DE. 2003. Mechanobiology and diseases of mechanotransduction. Ann Med 35(8):564–577.

Isenberg BC, Williams C, Tranquillo RT. 2006. Small-diameter artificial arteries engineered in vitro. Circ Res 98(1):25–35.

Joung IS, Iwamoto MN, Shiu YT, Quam CT. 2006. Cyclic strain modulates tubulogenesis of endothelial cells in a 3D tissue culture model. Microvasc Res 71(1):1–11.

Liu SQ. 1999. Biomechanical basis of vascular tissue engineering. Crit Rev Biomed Eng 27(1–2):75–148.

Liu M, Montazeri S, Jedlovsky T, Van Wert R, Zhang J, Li RK, Yan J. 1999a. Bio-stretch, a computerized cell strain apparatus for three-dimensional organotypic cultures. In Vitro Cell Dev Biol Anim 35(2):87–93.

Liu M, Tanswell AK, Post M. 1999b. Mechanical force-induced signal transduction in lung cells. Am J Physiol 277(4 Pt 1):L667–L683.

Ng CP, Swartz MA. 2003. Fibroblast alignment under interstitial fluid flow using a novel 3-D tissue culture model. Am J Physiol Heart Circ Physiol 284(5):H1771–H1777.

Ng CP, Swartz MA. 2006. Mechanisms of interstitial flow-induced remodeling of fibroblast-collagen cultures. Ann Biomed Eng 34(3):446–454.

Ng CP, Helm CL, Swartz MA. 2004. Interstitial flow differentially stimulates blood and lymphatic endothelial cell morphogenesis in vitro. Microvasc Res 68(3):258–264.

Ng CP, Hinz B, Swartz MA. 2005. Interstitial fluid flow induces myofibroblast differentiation and collagen alignment in vitro. J Cell Sci 118 (Pt 20):4731–4739.

Park JS, Huang NF, Kurpinski KT, Patel S, Hsu S, Li S. 2007. Mechanobiology of mesenchymal stem cells and their use in cardiovascular repair. Front Biosci 12:5098–5116.

Paszek MJ, Zahir N, Johnson KR, Lakins JN, Rozenberg GI, Gefen A, Reinhart-King CA, Margulies SS, Dembo M, Boettiger D, Hammer DA, Weaver VM. 2005. Tensional homeostasis and the malignant phenotype. Cancer Cell 8(3): 241–254.

Pedersen JA, Swartz MA. 2005. Mechanobiology in the third dimension. Ann Biomed Eng 33(11):1469–1490.

Raeber GP, Mayer J, Hubbell JA. 2008. Part I: A novel in-vitro system for simultaneous mechanical stimulation and time-lapse microscopy in 3D. Biomech Model Mechanobiol 7(3):203–214.

Ramanujan S, Pluen A, McKee TD, Brown EB, Boucher Y, Jain RK. 2002. Diffusion and convection in collagen gels: Implications for transport in the tumor interstitium. Biophys J 83(3):1650–1660.

Rivron NC, Liu JJ, Rouwkema J, de Boer J, van Blitterswijk CA. 2008. Engineering vascularised tissues in vitro. Eur Cell Mater 15:27–40.

Roeder BA, Kokini K, Sturgis JE, Robinson JP, Voytik-Harbin SL. 2002. Tensile mechanical properties of three-dimensional type I collagen extracellular matrices with varied microstructure. J Biomech Eng 124 (2):214–222.

Rutkowski JM, Swartz MA. 2007. A driving force for change: Interstitial flow as a morphoregulator. Trends Cell Biol 17(1):44–50.

Sacks MS, Yoganathan AP. 2007. Heart valve function: A biomechanical perspective. Philos Trans R Soc Lond B Biol Sci 362(1484):1369–1391.

Setton LA, Chen J. 2004. Cell mechanics and mechanobiology in the intervertebral disc. Spine 29(23):2710–2723.
Shieh AC, Athanasiou KA. 2003. Principles of cell mechanics for cartilage tissue engineering. Ann Biomed Eng 31(1):1–11.
Sorkin AM, Dee KC, Knothe Tate ML. 2004. ''Culture shock'' from the bone cell's perspective: Emulating physiological conditions for mechanobiological investigations. Am J Physiol Cell Physiol 287(6):C1527–C1536.
Soulhat J, Buschmann MD, Shirazi-Adl A. 1999. A fibril-network-reinforced biphasic model of cartilage in unconfined compression. J Biomech Eng 121(3):340–347.
Swartz MA, Fleury ME. 2007. Interstitial flow and its effects in soft tissues. Annu Rev Biomed Eng 9:229–256.
Tschumperlin DJ, Drazen JM. 2006. Chronic effects of mechanical force on airways. Annu Rev Physiol 68:563–583.
Vanepps JS, Vorp DA. 2007. Mechano-pathobiology of atherogenesis: A review. J Surg Res 142(1):202–217.
Voge CM, Kariolis M, MacDonald RA, Stegemann JP. 2008. Directional conductivity in SWNT-collagen-fibrin composite biomaterials through strain-induced matrix alignment. J Biomed Mater Res A 86(1):269–277.
Wang JH, Thampatty BP, Lin JS, Im HJ. 2007. Mechanoregulation of gene expression in fibroblasts. Gene 391(1–2):1–15.
Wipff PJ, Rifkin DB, Meister JJ, Hinz B. 2007. Myofibroblast contraction activates latent TGF-beta1 from the extracellular matrix. J Cell Biol 179(6):1311–1323.
Wirtz HR, Dobbs LG. 2000. The effects of mechanical forces on lung functions. Respir Physiol 119(1):1–17.
Wozniak MA, Desai R, Solski PA, Der CJ, Keely PJ. 2003. ROCK-generated contractility regulates breast epithelial cell differentiation in response to the physical properties of a three-dimensional collagen matrix. J Cell Biol 163(3):583–595.